Supplementary materials

S1 Metabarcoding

Dinoflagellate reads were often dominant in both systems (Fig. S1). We decided to not incorporate the dinoflagellate data in this phytoplankton-focused study for a number of reasons. First, it is known that many dinoflagellates are heterotrophic and/or mixotrophic. Gómez (2012), based on an analysis of 2,377 dinoflagellate species, reported that ~58% of marine dinoflagellates are heterotrophic, while the plastid-containing taxa are not necessarily strictly autotrophic, as most are considered mixotrophic (Jeong et al., 2010; Hansen, 2011). Both mixotrophic and heterotrophic dinoflagellates are also common components of Arctic plankton communities (Stoecker et al., 2017). Second, insufficient taxonomic resolution hindered reliable discrimination among phototrophic, heterotrophic, and mixotrophic dinoflagellates, with 56.8% of Dinophyceae ASVs remaining unclassified at the genus level (Fig. S2). Finally, the importance of dinoflagellates in metabarcoding data sets is likely inflated by high rRNA gene copy numbers (Lin et al., 2006; Ruvindy et al., 2023), a methodological bias previously reported for the same region, including NK fjord, where metabarcoding results contrasted with substantially lower abundances inferred from microscopy (Rodríguez-Marconi et al., 2024). For these reasons, we decided to only report pigment-based information which allowed unambiguous identification of phototrophic/mixotrophic dinoflagellates, i.e. peridinin, to evaluate the occurrence of photosynthetic dinoflagellates in our study systems.

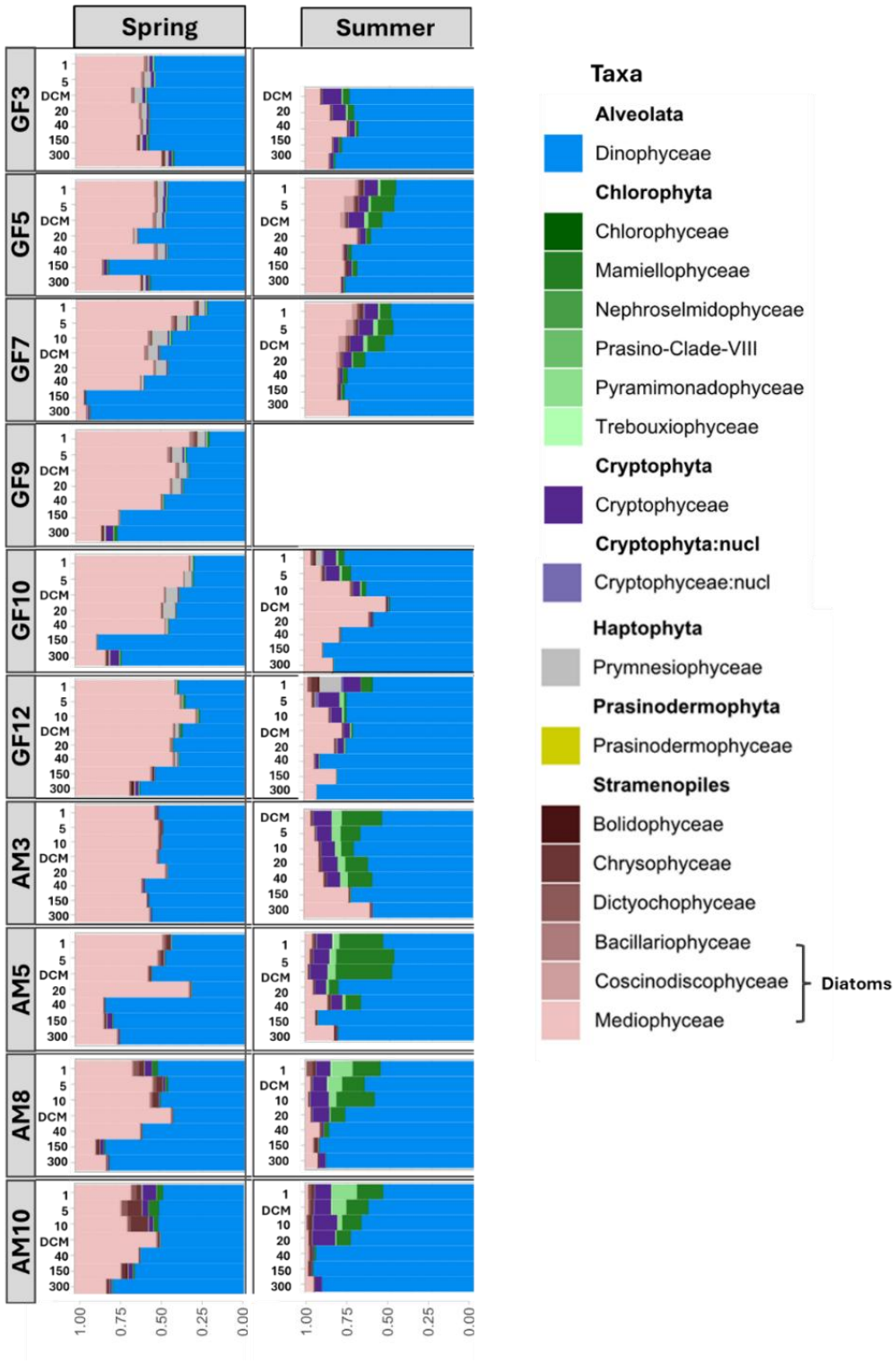

Figure S1: *Phytoplankton (including Dinophyceae) relative abundances based on metabarcoding data at discrete sampling depths and stations in NK (GFx) and AM (AM) in spring (left) and summer (right), from the outer (GF3, AM3) to the inner fjord (GF12, AM10). DCM indicates deep chlorophyll maximum. The diatom group is delineated with a bracket.*

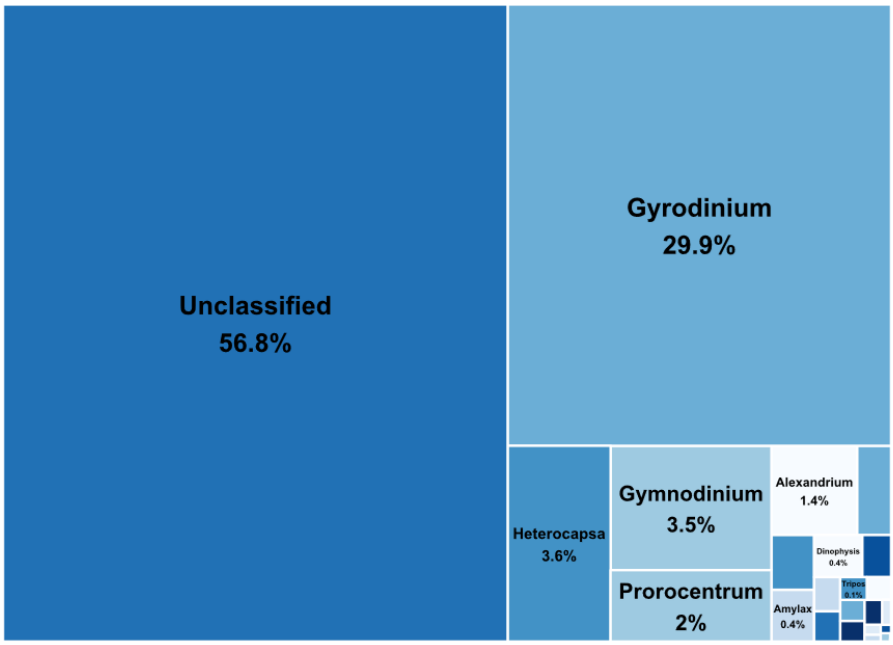

Figure S2. *Treemap showing the relative abundance (%) of Dinophyceae genera across all samples. The area of each rectangle is proportional to the total number of sequences assigned to each genus. Percentages indicate the contribution of each genus to the total Dinophyceae reads.*

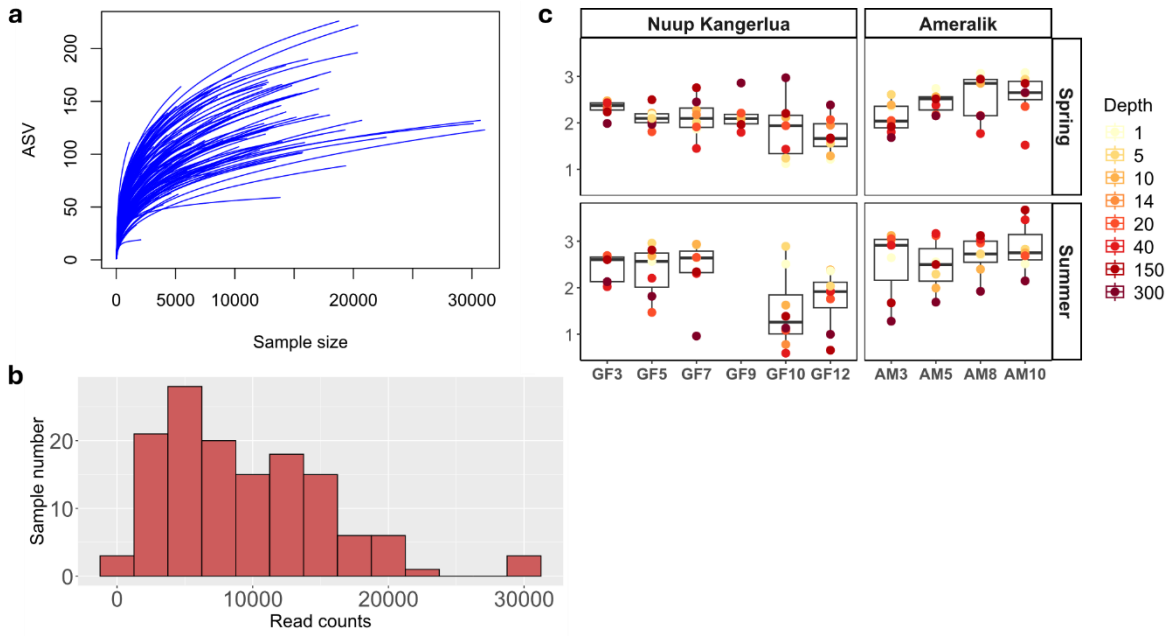

Figure S3: *(a) Rarefaction curves of phytoplankton metabarcoding data (V4 18S). (b) Bar plots showing the distribution of sequencing depth across samples. (c) Boxplots of Shannon diversity based on phytoplankton data rarefied to the minimum sample size at stations in NK (GFx, left) and AM (AMx, right) in spring (top) and summer (bottom), from the outer (GF3, AM3) to the inner fjord (GF12, AM10). Colored dots indicate discrete sampling depths, and solid black lines represent the median value for each station.*

S2 Environmental data

Table S1. *Sampling locations, including fjord, station name, geographic coordinates (latitude and longitude), sampling date, and depth (m) of the deep chlorophyll maximum (DCM).*

Fjord	Station	Latitude	Longitude	Data	DCM
Nuup Kangerlua	GF3	64.1167	-51.8833	20.08.2021	10
Nuup Kangerlua	GF5	64.2667	-51.6667	24.08.2021	10
Nuup Kangerlua	GF7	64.425	-51.51	24.08.2021	10
Nuup Kangerlua	GF10	64.61	-50.9583	23.08.2021	14
Nuup Kangerlua	GF12	64.715	-50.5467	23.08.2021	14
Ameralik	AM3	64.0552	-51.4973	27.08.2021	1
Ameralik	AM5	64.0947	-51.1891	27.08.2021	10
Ameralik	AM8	64.1734	-50.7546	26.08.2021	5
Ameralik	AM10	64.184	-50.4324	26.08.2021	5
Nuup Kangerlua	GF3	64.1167	-51.8833	11.05.2022	10
Nuup Kangerlua	GF5	64.2667	-51.6667	11.05.2022	10
Nuup Kangerlua	GF7	64.425	-51.51	17.05.2022	14
Nuup Kangerlua	GF9	64.5667	-51.1667	17.05.2022	10
Nuup Kangerlua	GF10	64.61	-50.9583	19.05.2022	10
Nuup Kangerlua	GF12	64.715	-50.5467	19.05.2022	14
Ameralik	AM3	64.0552	-51.4973	01.06.2022	14
Ameralik	AM5	64.0947	-51.1891	01.06.2022	14
Ameralik	AM8	64.1734	-50.7546	30.05.2022	20
Ameralik	AM10	64.184	-50.4324	30.05.2022	20

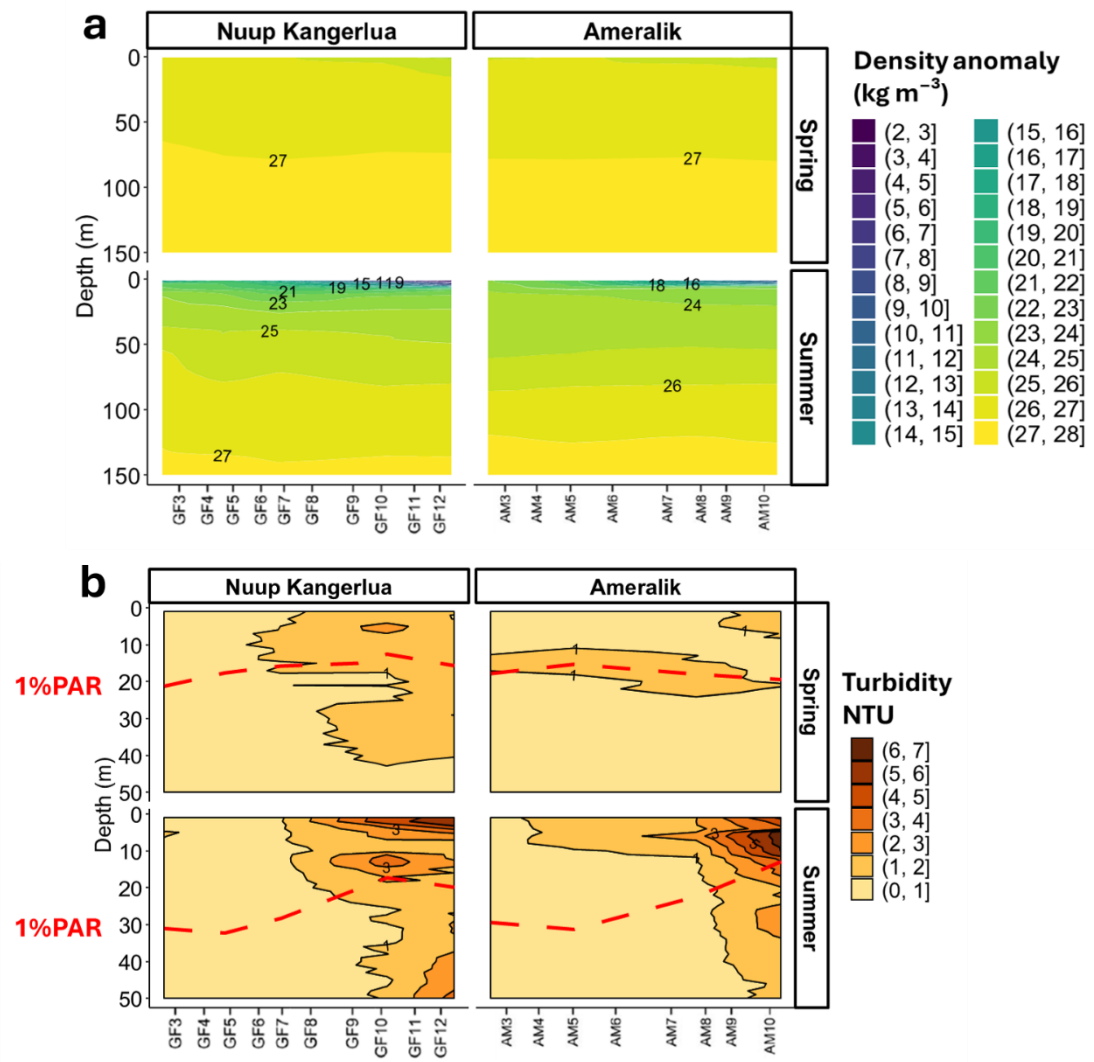

Figure S4. *(a) Vertical sections of density anomaly (σθ, kg m⁻³) for transects in Nuup Kangerlua (NK) and Ameralik (AM) during spring (top) and summer (bottom), extending from the surface to 150 m depth. (b) Close-up of turbidity (NTU) profiles for the same transects and seasons, restricted to the upper 50 m of the water column. In both panels, stations are arranged from the outer to the inner fjord and station locations are indicated along the x-axis. The red dashed line in panel (b) indicates the depth at which photosynthetically active radiation (PAR) is reduced to 1% of its surface value, marking the lower limit of the euphotic zone.*

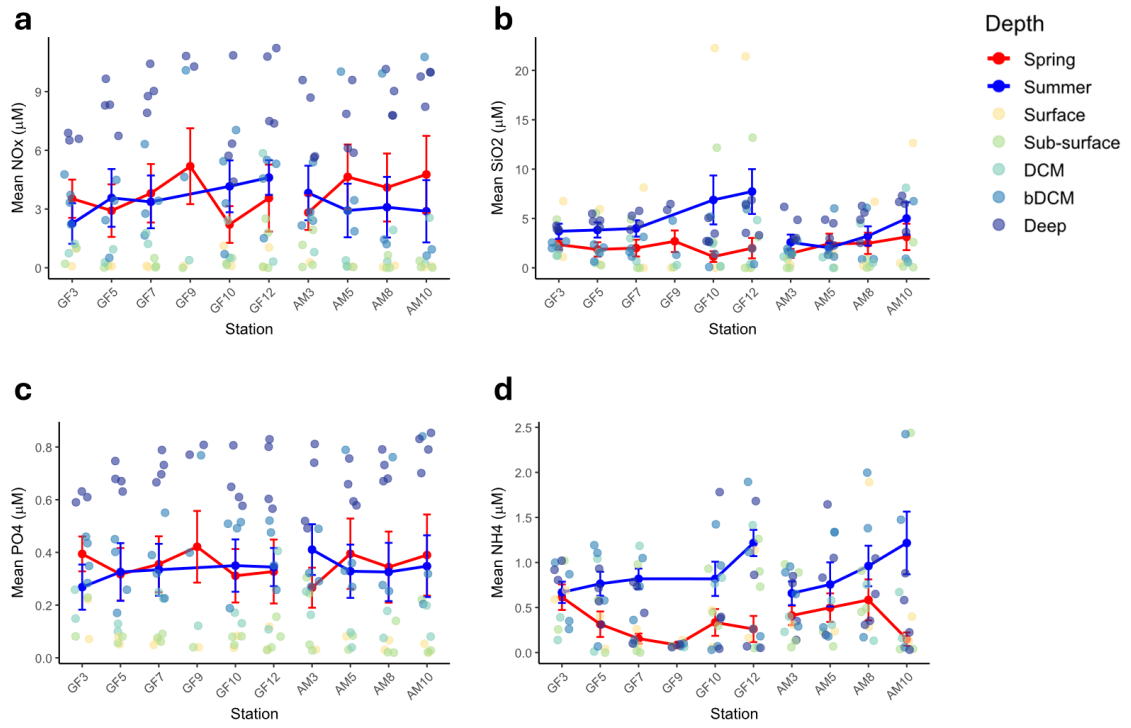

Figure S5: *Mean concentrations (µM) of (a) NOx, (b) SiO_2, (c) PO_4^{3-}, and (d) NH_4^+ by station in spring (red) and summer (blue). Error bars represent ± standard deviation. Dots represent individual measurements. Sampling depths include: Surface (1 m), Sub-surface (5–10 m), DCM (Deep Chlorophyll Maximum), bDCM (20–40 m), and Deep (150–300 m).*

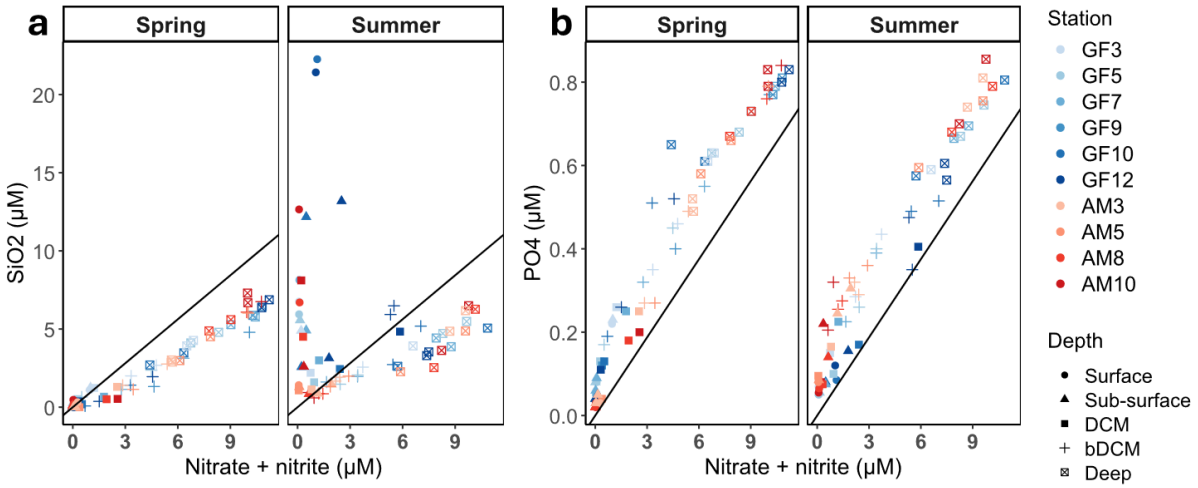

Figure S6: *(a) Silicate (SiO_2) vs. nitrate + nitrite ($NO_3^- + NO_2^-$) and (b) phosphate (PO_4^{3-}) vs. nitrate + nitrite concentrations (µM) at sampled stations and depths during spring and summer. Sampling depths include: Surface (1 m), Sub-surface (5–10 m), DCM (Deep Chlorophyll Maximum), bDCM (20–40 m), and Deep (150–300 m). Black lines indicate the Redfield-Brzezinski molar ratios (C:Si:N:P = 106:15:16:1), based on Redfield (1934, 1958) and Brzezinski (1985).*

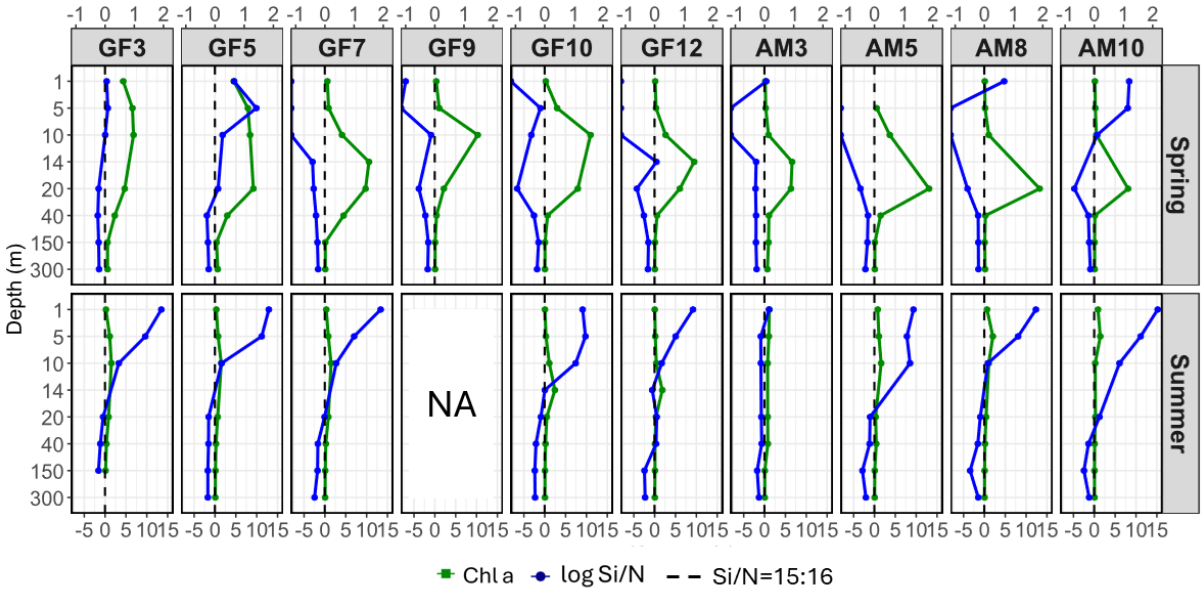

60

61 ***Figure S7:*** *Depth profiles of chlorophyll a (Chl a, µg L^{-1}, green line, bottom scale), logarithm of Si/N*
62 *ratio (blue line) and Redfield stoichiometry (Si/N = 15:16, dashed line, top scale) in NK (GFx) and*
63 *AM (AMx) in spring (top) and summer (bottom).*

S3 iFCM and FlowCAM

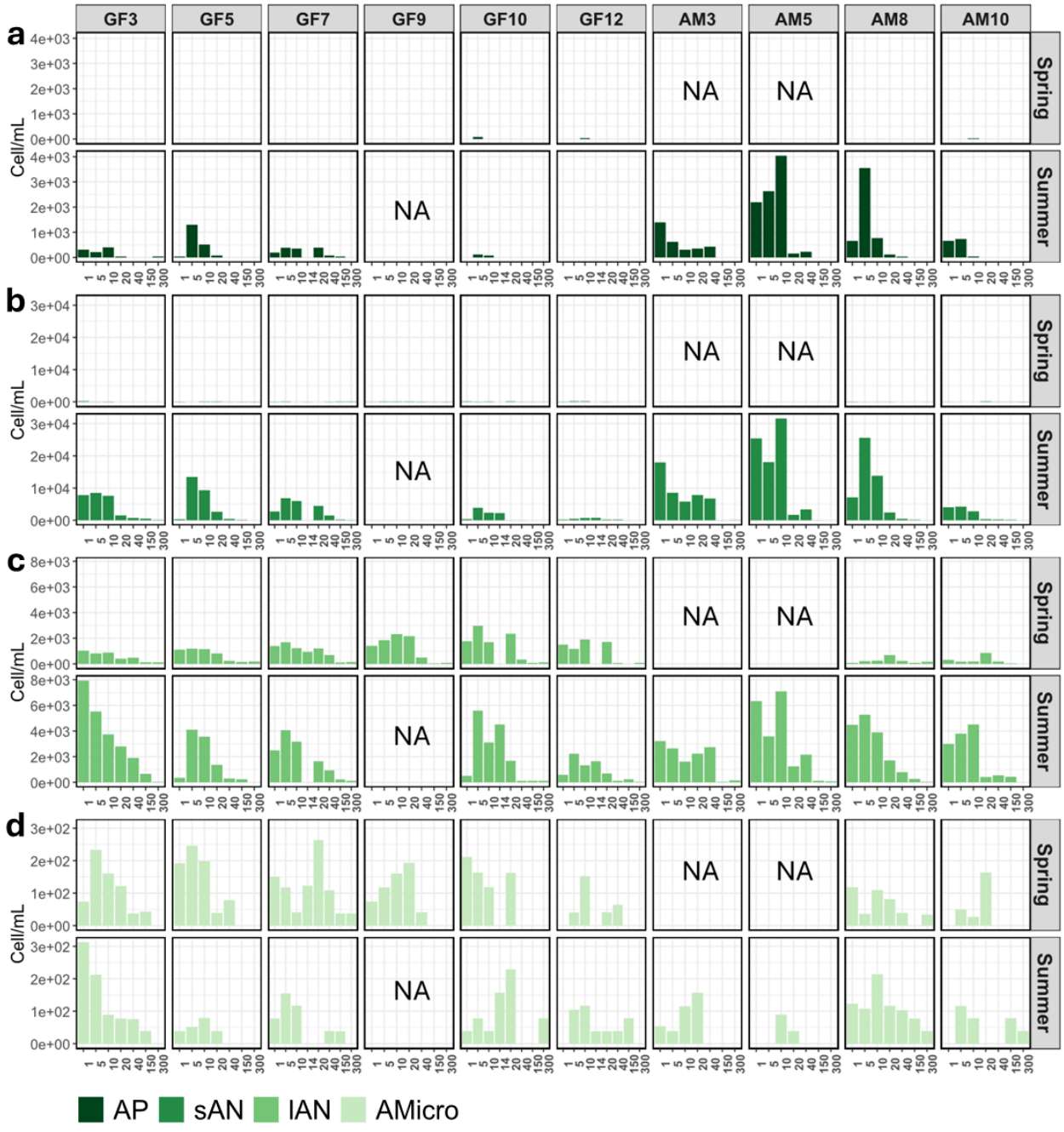

Figure S8: *(a-b-c-d) Bar plots of microbial abundances (cells mL^{-1}) at discrete sampling depths in NK (GFx) and AM (AMx) in spring (top) and summer (bottom). (a) AP – picophytoplankton, dark green; (b) sAN – small nanophytoplankton, medium green; (c) lAN – large nanophytoplankton, light green; (d) AMicro – microphytoplankton, pale green. DCM = deep chlorophyll maximum. Note different scale of y-axis. NA – data not available.*

In spring, phototrophic picoplankton (AP) and small phototrophic nanoplankton (sAN) were virtually absent (Fig. S8a, b). Numbers of large phototrophic nanoplankton (lAN) were highest at GF10 (~2 x 10^3 cells mL^{-1}, upper 40 m) and lowest in inner AM (~300 cells mL^{-1}, upper 40 m; Fig. S8c). Microphytoplankton (AMicro) abundance ranged between 100–200

cells mL^{-1} (Fig. S8d), but most diatom colonies (>100 µm) would have been eliminated during prefiltration (see FlowCAM).

In summer, AP was present at all stations except GF12, peaking at ~4 x 10^3 cells mL^{-1} at the DCM in AM5. Average AP concentrations in the upper 40 m were higher in AM (~1 x 10^3 cells mL^{-1}) than in NK (Fig. S8a). sAN and lAN were most abundant in AM5 and AM8, averaging ~1,3 x 10^4 and ~4 x 10^3 cells mL^{-1}, respectively, in the upper 40 m (Fig. S8b-c). In NK, their concentrations were lower (sAN ~3 x 10^3 and lAN ~2,5 x 10^3 cells mL^{-1}), except at 1-5 m in GF3 where lAN reached the highest abundance (on average 6.7 x 10^3 cells mL^{-1}). AMicro was less abundant than in spring, averaging ~100 cells mL^{-1} in the upper 40 m of both fjords, except at GF3 (300 cells mL^{-1} at 1m; Fig. S8d).

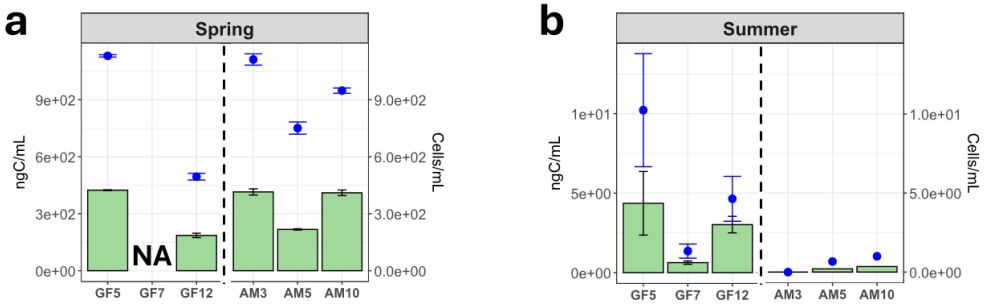

Figure S9: *Bars represent the total carbon biomass (ng/mL) of diatom colonies and the blue dots correspond to the second y-axis and indicate single cell abundances at DCM in (a) spring and (b) summer. Error bars represent +/- standard deviation. Data not available for GF7 spring (NA).*

S4 Pigments

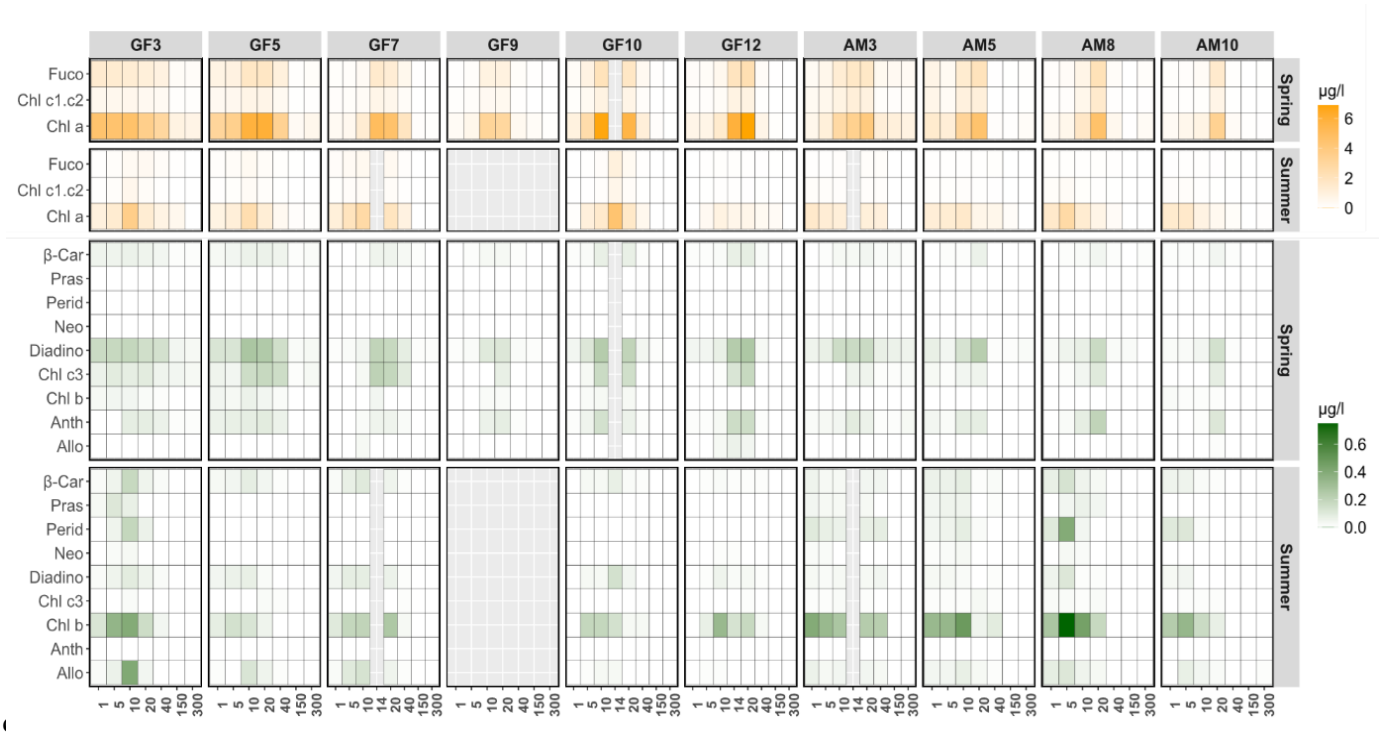

Figure S10: *Heatmap of pigment concentrations (µg L^{-1}) detected by HPLC analysis in NK (GFx) and AM (AMx) in spring (first and third panel) and summer (second and fourth panel). Pigments with lower concentrations (green): Allo = alloxanthin, Anth = antheraxanthin, Chl b = chlorophyll b, Chl c3 = chlorophyll c3, Diadino = diadinoxanthin, Neo = neoxanthin, Perid = peridinin, Pras = prasinoxanthin, β-Car = beta-carotene. Pigments with higher concentrations (orange): Chl a = chlorophyll a, Chl c1.c2 = chlorophyll c1 + c2, Fuco =fucoxanthin.*

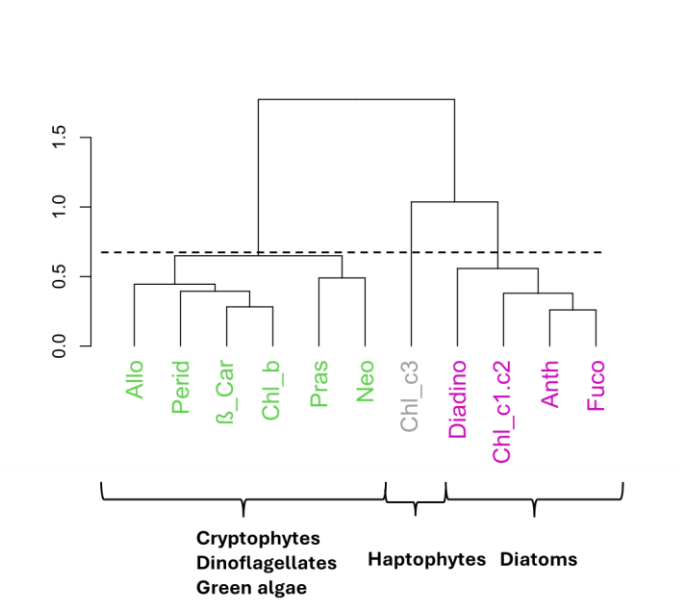

Figure S11: *Hierarchical clustering of phytoplankton pigment to TChla concentration ratios, showing three distinct taxonomic clusters using a linkage cutoff distance of 0.7 (dashed line). Diverse community (green color): cryptophytes, dinoflagellate, prasinophytes and chlorophytes (Green algae); haptophytes (grey color) and diatoms (magenta color).*

Hierarchical cluster analysis of pigment concentrations normalized to TChla across the two sampling seasons revealed three distinct phytoplankton pigment clusters at a linkage distance of 0.7 (Fig. S11). These pigment associations can be used to infer the likely taxonomic composition of each cluster (Tab. S2). The first cluster is composed of pigments typically associated with diatoms—Fuco, Anth, Diadino and Chl c1.c2—which exhibit strong mutual correlations and form a group distinct from all other pigments. Although Chl c1.c2 can be found in other groups such as dinoflagellates and haptophytes, its strongest correlation here is with pigments characteristic of diatoms, suggesting diatom dominance within this cluster. Chl c3 likely reflects the presence of haptophytes, in which it is often a dominant pigment (Higgins et al., 2011). The third cluster represents a combination of pigments indicative of different phytoplankton groups (diverse community): prasinophytes (Pras, Neo), chlorophytes (Chl *b*, β-Car), dinoflagellates (Perid), and cryptophytes (Allo). This group is clearly separated from the diatom–haptophyte cluster, suggesting a different community structure, likely reflective of summer assemblages. The clustering output is statistically robust: the cophenetic correlation coefficient—a measure of how well the dendrogram preserves original

pairwise distances—is high (0.94), and the associated p-value is very low ($\ll 0.001$), confirming that the dendrogram provides a significant and appropriate representation of the pigment relationships.

Table S2: *Summary of 11 pigments identified in this analysis and their distribution across 9 taxonomic groups. Adapted from Jeffrey et al., 2011. Pigment abbreviation: Allo = alloxanthin, Perid = peridinin, Diadino = diadinoxanthin, Fuco =fucoxanthin, Chl c1.c2 = chlorophyll c1 + c2, Chl c3 = chlorophyll c3, Anth = antheraxanthin, Neo = neoxanthin, Pras = prasinoxanthin, Chl b = chlorophyll b, β-Car = beta-carotene.*

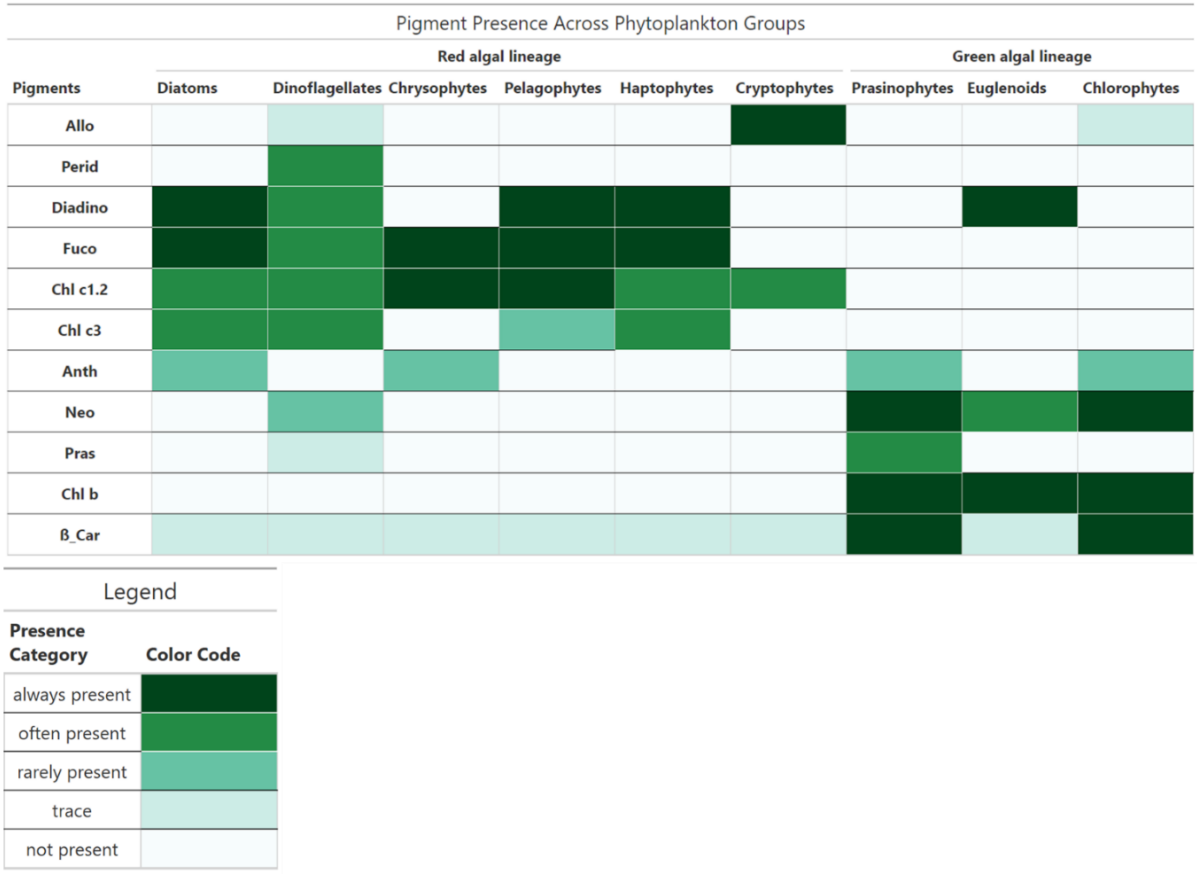

Table S3: *Pearson correlation results between each EOF mode and environmental variables. Turbidity variable not shown as never significant. Significance levels: *** $p \leq 0.001$, ** $p \leq 0.01$, * $p \leq 0.05$, ns = not significant.*

	Temperature	Salinity	Chlophyll a	PAR	NO_3+NO_2	PO_4	SiO_2	NH_4
Mode 1	0.67***	-0.48***	-0.21*	ns	ns	ns	ns	ns
Mode 2	ns	-0.39***	ns	-0.27**	0.23*	0.28**	0.48***	0.34***
Mode 3	ns	0.24*	0.55***	-0.36***	ns	ns	-0.21*	ns
Mode 4	ns	ns	ns	ns	ns	ns	ns	ns

Supplementary references

Gómez, F. (2012). A quantitative review of the lifestyle, habitat and trophic diversity of dinoflagellates (Dinoflagellata, Alveolata). Systematics and Biodiversity, 10: 267–275. Doi: 10.1080/14772000.2012.721021

Hansen, P. J. (2011). The role of photosynthesis and food uptake for the growth of marine mixotrophic Dinoflagellates. Journal of Eukaryotic Microbiology, 58: 203-214. Doi: 10.1111/j.1550-7408.2011.00537.x

Jeffrey, S. W., Wright, S. W., Zapata, M. (2011). Microalgal classes and their signature pigments. In S. Roy, C. A. Llewellyn, E. S. Egeland, G. Johnsen (Eds.). Phytoplankton Pigments: Characterization, Chemotaxonomy, and Application in Oceanography, 3–77. Cambridge, United Kingdom: Cambridge University Press.

Jeong, H. J., Yoo, Y. D., Kim, J. S., Seong, K. A., Kang, N. S., Kim, T. H. (2010). Growth, feeding and ecological roles of the mixotrophic and heterotrophic dinoflagellates in marine planktonic food webs. Ocean Science Journal, 45: 65–91. Doi: 10.1007/s12601-010-0007-2

Lin, S. (2006). The smallest dinoflagellate genome is yet to be found: a comment on Lajeunesse et al. “Symbiodinium (pyrrhophyta) genome sizes (DNA content) are smallest among dinoflagellates”. Journal of Phycology, 42: 746-748. Doi: 10.1111/j.1529-8817.2006.00213.x

Rodríguez-Marconi, S., Krock, B., Tillmann, U., Tillmann, A., Voss, D., Zielinski, O., Vásquez, M., and Trefault, N. (2024). Diversity of eukaryote plankton and phycotoxins along the West Kalaallit Nunaat (Greenland) coast. Frontiers in Marine Science, 11: 1443389. Doi: 10.3389/fmars.2024.1443389

Ruvindy, R., Barua, A., Bolch, C. J. S. Sarowar, C., Savela, H., Murray, S. A. (2023). Genomic copy number variability at the genus, species and population levels impacts in situ ecological analyses of dinoflagellates and harmful algal blooms. ISME Communications, 3: 70. Doi: 10.1038/s43705-023-00274-0

Stoecker, D. K., Hansen, P. J., Caron, D. A., and Mitra, A. (2017). Mixotrophy in the marine plankton. Annual Review of Marine Science, 9: 311–335. Doi: 10.1146/annurev-marine-010816-060617